



EARTH OBSERVATION AND GEOMATICS ENGINEERING

website: <https://eoge.ut.ac.ir>

Monitoring of sea surface currents by using sea surface temperature and satellite altimetry data in the Caspian Sea

Emad Ghalenoeei¹, Mahdi Hasanlou^{2*}

¹Department of Geomatics Engineering, University of Calgary, Calgary, Alberta, Canada

²School of Surveying and Geospatial Engineering, College of Engineering, University of Tehran, Tehran, Iran

Article history:

Received: 25 December 2016, Received in revised form: 28 March 2017, Accepted: 1 May 2017

ABSTRACT

The spatial and temporal monitoring of Sea Surface Currents (SSCs) has a crucial importance in the study of the strategic environmental assessments. Although the geostrophic currents have been calculated by altimetry data, in this study, we show these currents have an appropriate correlation with the Sea Surface Temperature (SST). Two different methods are used to estimate the SSCs. First, we propose a model for calculating the geostrophic currents via removing the effects of Mean Sea Surface (MSS) from the Sea Surface Height (SSH), and second, the optical flow method (Horn-Schunck) has been applied to two sequential SST imageries to extract the SST patterns movements. In the first part of results, we map the geostrophic currents on the SST surface to explain the physical events like eddies, and in the second part, we calculate the optical flow and compare them with the geostrophic currents. Because there are no appropriate validation currents in the Caspian Sea, we use the SST products corrected by NASA and no changes have been performed on them in this study. We conclude that both optical flow and geostrophic currents show the same results but in different schemes. The schematic results shown in this article can provide new and small-scale phenomena to see that movements of sea surface have meaningful aspects.

KEYWORDS

Sea surface currents
Sea surface-temperature
Satellite altimetry
Optical flow
Geostrophic-currents

1. Introduction

Sea Surface Currents (SSCs) provide a unique opportunity to understand the dynamics of the sea. They include separate parts that have their own particular names; water in motion is called a current; the direction toward which it moves is called set, and its speed is called the draft. (Bowditch, 2012). The usefulness of the SSCs monitoring for large-scale and local-scale studies is well established, as demonstrated by studies of the ocean circulation models, diversity of events like the circulation, its energetics, driving forces, characteristic fluxes, dynamical balances, ventilation and mixing, and the type and structure of its changeability, among many other questions (Stammer et al., 2003). In addition to in situ data, a variety of satellite data such as the Sea Surface Temperature (SST) imageries and altimetry data can be utilized at the same time for describing the Sea

Surface Currents (SSCs) and their other phenomena like vortex and eddies structures in the sea and oceans (Cohen & Herlin, 1996). The important question that we will explain in this article is what correlation exists between different SSCs calculated by separate satellite data. Furthermore, the SSCs processes are more difficult to resolve within in situ data, because of two types of problems. First, and most significantly, the limitations of temporal and spatial resolutions do not allow us to calculate precise SSCs. Second, collecting in situ data need to spend much cost and time. Thus, satellite data are firmly more useful in the SSCs processes and in this work we use SST images and satellite altimetry data, which include Sea Surface Height (SSH) and Mean Sea Surface (MSS). The distance between satellite and sea surface is measured by Radar Altimetry (Vignudelli et al., 2011). This measured distance by the satellite is called

* Corresponding author

E-mail addresses: emad.ghalenoeei@ucalgary.ca (E. Ghalenoeei); hasanlou@ut.ac.ir (M. Hasanlou)

DOI: 10.22059/eoge.2017.226309.1001

the range, the position of a satellite that is known exactly from its orbit then the absolute elevation of the sea surface is calculated from the difference between the orbit altitude and the range (Vignudelli et al., 2011). Behind satellite data advantages they have own limitations, for example, we cannot use the SST imageries taken by MODIS sensor in cloudy weather (Brian B. Barnes, 2013 ; Ghalenoei et al., 2015). Contrary to MODIS sensor, Altimetry satellites can calculate the SSH in this situation, but their data do not have acceptable spatial resolutions. One of the methods to address the problems described above is to increase the number of satellites deployed to produce gridded SSH where this makes the estimated SSCs extremely accurate (Saraceno et al., 2008). The complexity of the SSCs is revealed by patterns of SST (Minnett et al., 2004) and a lot of events such as eddies and jet currents can be cleared in SST maps especially in coastal areas (Ghalenoei et al., 2017 ; Vignudelli et al., 2011). To explain more, the SST does not have any significant effect on the SSCs, but by tracing the SST patterns via optical flow methods, extracting sea surface motion patterns is possible, because the SSCs influence the SST patterns (Martin Gade, 2012;Cohen & Herlin, 1996;M. Hasanlou & M. R. Saradjian, 2006), (Jin et al., 2001). In this study, we downloaded MODIS SST products to investigate the SST imageries, which contain measurements of ocean color and SST for oceanographic applications (Minnett et al., 2004). The SSCs are extracted from the SST imageries by utilizing optical flow method and Horn-Schunck algorithm (Horn & Schunck, 1981). In previous studies, Marcello used two methods of region matching algorithm and differential algorithm based on Lucas Kanadeh and Black-Anandan techniques (Marcello et al., 2007). The first disadvantage of region matching is that the template window size must be large to have sufficient correlations; secondly, it is not able to generate motion vectors if the values of minimum or maximum are the same in multimodal matching surfaces. To use the cross-correlation method that was suggested by (Seppke et al., 2012), one needs to estimate a global motion to be able to extract the local motions. In addition, if there is a big structural change in the images features, this method may fail (Seppke et al., 2012). The Horn method that is used in this article needs no interpolation and global motion and it can create smooth currents. Although the satellite altimetry is not able to monitor such small-scale coastal phenomena directly (Vignudelli et al., 2011), in the present study, the geostrophic currents calculated from altimetry data have enough correlation with the SST maps, and it demonstrates that the proposed method for estimating the geostrophic currents and selected altimetry data are appropriate. This article is organized as follows: In section 2, the proposed methods used to calculate the SSCs are explained, the same as Horn and Schunck (optical flow), Thin Plate Spline (TPS) and the geostrophic equations. In section 3, the SST and satellite altimetry data are presented, and the Sea Level Anomaly (SLA) is estimated from them. In section 4, both optical flow and geostrophic currents are compared to each other, and firm criterion for validation is the SST surface maps because SST products downloaded and no processes

and no changes have been performed on them, in other words, the SST can show an eddy by showing rotating patterns. So the SST maps play the role of a validation for the optical flow vectors and geostrophic currents. A discussion of the results, their limitations, and possible future expansion conclude the article in section 5.

2. Methods

2.1 Optical flow (Horn-Schunck)

The optical flow estimates the motions of each pixel in two dimensions imageries (Barron et al., 1994), and one of the usages is calculating the motions of SST patterns in SST imageries when two sequential SST imageries input to this method (M. Hasanlou & M. R. Saradjian, 2006). Horn and Schunck algorithm is one of the optical flow methods used in this article, and it has a smoothness parameter for changing the SSCs schemes and making them more appropriate.

Consider that value of each pixel or each point with image coordinates (x, y) at time t is marked by $I(x, y, t)$. Horn and Schunck supposed that value of a special point in the SST pattern is constant (if time interval between images is short), because of that it can find its matches in the second image, then the motion vector of that point is calculated by two components (u, v) (Horn & Schunck, 1981). In other words, the SSCs just change the position of SST patterns and values of SST patterns do not change; this means that diurnal variation of SST is usually very small (Kawai & Wada, 2007). So the first step for optical flow process is equation (1) that supposes to have constant SST patterns (Horn & Schunck, 1981);

$$\frac{dI}{dt} = 0 \quad (1)$$

where, I is pixel value of the SST image and t is time. The equation of flow that is represented by E , is like a global energy functional which is tried to be minimized (Horn & Schunck, 1981).

$$E = \iint [(I_x u + I_y v + I_t)^2 + \alpha^2 (\|\nabla u\|^2 + \|\nabla v\|^2)] dx dy \quad (2)$$

where, I_x , I_y and I_t are the derivatives of image brightness values along x , y and time dimensions respectively, u and v are velocity of optical flow results and the parameter α is a constant for regularization. If α gets larger values, the flows will lead to be smoother (Horn & Schunck, 1981). In this study, α is 3 and other parameters (derivatives of image brightness) are calculated via central difference operator.

2.2 Thin Plate Spline (TPS)

Altimetry data (CorrSSH) used in this work are along-track and calculating the SSCs requires regular grids of SSH. So, the CorrSSH data are merged and interpolated by Thin Plate Spline (TPS) method to provide these grids. In previous studies, some applications in oceanography such as interpolating satellite altimeter data were carried out (Vennell & Beatson, 2009) and TPS was used to make accurate sea surface topography maps from satellite altimetry data (Sandwell, 1987). The answer of TPS algorithm is in this form:

$$F(x,y)=a_0+a_1x+a_2y+\sum_{i=1}^n \lambda_i r_i^2 \log r_i \quad (3)$$

$$r_i^2=(x-x_i)^2+(y-y_i)^2 \quad (4)$$

where, a_0 , a_1 and a_2 are the coefficients of the spline planar term and λ_i is the coefficient for the i^{th} term of spline, (x_i, y_i) are distinct control points coordinates and $F(x, y)$ is the value of estimation at a given point (x, y) . To estimate the SSH grid and Mean Sea Surface (MSS) grid, the TPS is executed once for SSH and once for MSS Separately.

2.3 Geostrophic Equations

In this study, the geostrophic currents are estimated based on Sea Level Anomaly (SLA) calculated by removing the effects of MSS from SSH. After performing TPS, both grids (SSH and MSS) have the same size and overlap completely according to their coordinates, so we produce the SLA in grid form. The east and north velocity components of these currents at a given grid point are estimated by using centered differences as:

$$u_s = -\frac{g}{f} \frac{\partial SLA}{\partial y}; \quad v_s = \frac{g}{f} \frac{\partial SLA}{\partial x} \quad (5)$$

where, SLA is the Sea Level Anomaly grid, x and y are direction in of Cartesian coordinate system, g is the gravity acceleration and f is Coriolis parameter, which is $f=2\Omega \sin \varphi$, Ω is earth's rotational rate (7.292115×10^{-5} radian/s), φ is latitude (Stewart, 2009) and u_s and v_s are the east and north velocity components of geostrophic currents, respectively.

3. Dataset

3.1 The Caspian Sea

The domain considered in this work is the Caspian Sea (36° to 47° N and 46° to 54° E) which is a completely surrounded, landlocked body of water on the continent of the Euro-Asian (Gunduz & Özsoy, 2014). It is the largest and greatest lake on the earth and bigger than the Great American lakes and Lake Victoria in Africa due to surface area (Aladin & Plotnikov, 2004). The ecological system in the Caspian Sea area has been in a weighty manner changed by anthropogenic actions, mostly as a reason of alterations in the water circulation and degradation of the water attribute in the ecological system (Barannik et al., 2004).

3.2 SST Imageries

Tracing the temperature patterns by optical flow method leads us to diagnose the SSCs. In other words, we extract SSCs by tracing surface temperature. The SST products are obtained from NASA website (the National Aeronautics and Space Administration). Terra and Aqua are two sun-synchronous satellites having visible and infrared radiometers onboard in MODIS sensor. Altitudes of these satellites are 705 km from mean sea level. They have $\pm 55^\circ$ scanning angle covering 2330 km swath width providing global daily coverage. Terra is a descending satellite with descending pass in the morning at 10:30 AM and Aqua is an ascending satellite with an ascending pass in the afternoon at 1:30 PM. In general, MODIS sensor includes 36 spectral

bands ranging from 0.4–14.4 μm (Hosoda et al., 2007). These products are gridded and their resolutions are 250 m at nadir, with five bands at 500 m; the resolution of the remaining 29 bands is 1 km. MODIS sensor calculates SST in nearly 11 μm band (“MODIS Web”, 2016). To extract the SSC from SST, we need one or more pair/successive imageries. The revisit cycle of these satellites (Aqua and Terra) is almost 12 hours. Selection of SST imageries with minimum time span for Optical flow process is an important factor. So in this work, we selected three SST imageries. First, an SST image is taken by Aqua on 30 July 2010 at 22:40, and geostrophic currents consideration to this SST image time are calculated and mapped on SST surface. Two other imageries are two sequential SST imageries with minimum and appropriate time difference between them. They are taken by Aqua on 2 August 2010 at 09:35 and 23:10, so time difference between them is almost 11 hours. However, finding SST imageries without cloud covering is a basic problem especially in the Caspian Sea but in this work, we selected the best and the most appropriate SST imageries for Optical flow process.

3.3 Satellite Altimetry Data

The types of satellite altimetry data used in the present study are along-track SSH and MSS data, both downloaded from the AVISO FTP site (data are available at <ftp://ftp.cls.fr>). These data are corrected and processed by Archiving, Validation, and Interpretation of Satellite Oceanographic Data (AVISO), in France (AVISO, 2016) and they are known as CorrSSH data. To cover the gaps between altimetry tracks, we used multi-mission altimetry data (Jason-1, Jason-2, and Envisat). The most difference between these missions is their repeat cycles and tracks or passes; repeat cycle of Envisat (~35 days) is more than Jason-1 and Jason-2 (~10 days) but the distance between the passes for Envisat is less than the two other missions. However, the most important factor to make the SSH grid is time. Because in a short time span (one day) there are not enough altimetry passes or data so in this work and for the first part of the results, we selected altimetry data for two days before and two days after 30 July 2010 (5 days), and this criterion refers to the SST image time (on 30 July 2010). Because in this article, we compare the optical flow to geostrophic currents, for the second part of the results, the altimetry data date has to be close to the SST Imageries date. Two sequential SST Imageries were taken on 2 August 2010 (one of them in the morning and the other at night) so altimetry data from 31 July 2010 to 4 August 2010 are selected, and the SSH grids are calculated by them.

4. Results

4.1 Geostrophic currents and SST surface

All the results in this part are calculated by altimetry along-track data from multi-missions in the period of five days (2010-07-28 to 2010-08-01) and mapped on SST that was taken by Aqua satellite on 30 July 2010 at 22:40. Figure 2 shows the geostrophic currents that mapped on SST surface. It is an eddy which circles near the coast and this eddy does not allow colder water of the coast to enter its center, therefore, colder water circles around this eddy and

also there are some currents which move along the coast toward the south that is known as along-shore currents (Vignudelli et al., 2011). The SST map of the Caspian Sea is a unique combination of cold and warm waters that move to each other with different SSCs (Vignudelli et al., 2011), in order that they do not combine with themselves very fast, so they show different SSCs which carry cold or warm water can be obvious in SST maps (Vignudelli et al., 2011). In Figure 3a, the SST map of a local area on the eastern coast of the Caspian Sea is shown. The southern regions of the Caspian Sea are usually warmer than the eastern and middle regions of it; this leads us to identify two different SSCs. For instance, the SSCs which carry the warm water of the

southern regions move and enter the cold water of the eastern coastal areas and without calculating the geostrophic currents, it can be clear from SST map, to prove this movement, the geostrophic currents were estimated. Figure 3-a shows geostrophic currents that mapped on SST surface. Parts of warm water in the southern areas move toward the north (on a straight line along the coast), furthermore, geostrophic currents show this straight line toward the north. Another point is that SLA contours (especially the zero contour line of SLA) are almost the straight lines in this region (Figure 3b).

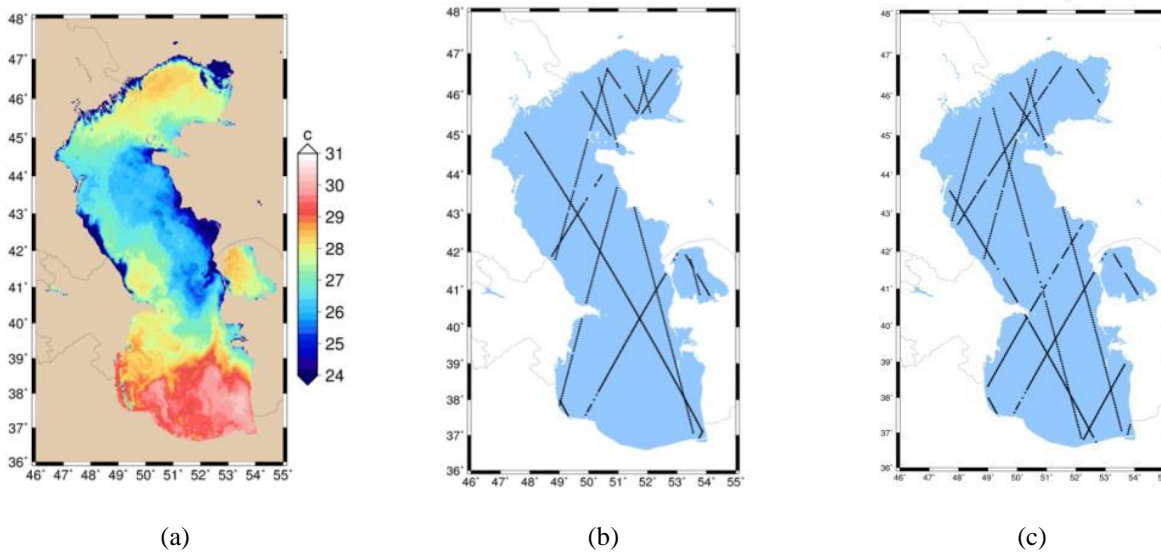


Figure 1. (a) SST image was taken by Aqua on 30 July 2010 at 22:40, (b) Altimetry along-track data from multi-missions in the period of five days (2010-07-28 to 2010-08-01), and (c) Altimetry along-track data from multi-missions in the period of five days (2010-07-31 to 2010-08-04)

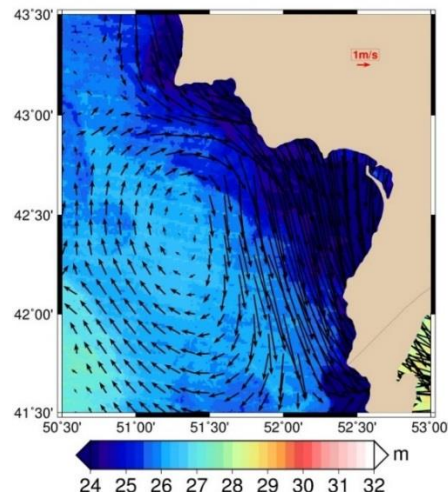


Figure 2. Geostrophic currents are mapped on SST surface. The SST was taken by Aqua satellite on 30 July 2010 at 22:40

One of the events that happens frequently in the eastern coastal areas in the Caspian Sea is upwelling of cold waters, which moves up from the depth and is visible on the sea surface (Vignudelli et al., 2011). One of the upwelling areas is selected and shown in Figure 4, and the aim is to determine

cold waters movements produced by the upwelling phenomena. To investigate water movements from SST map, some specific areas are numbered. The number 1 area (shown in Figure 4a) is a region near the coast that upwelling occurred and there is a high density of cold waters there and

spread by surface currents, in addition, tracing these waters causes to identify the SSCs directions. The cold waters of the number 1 move toward the sea and divided into numbers 2 and 3. Furthermore, the estimated geostrophic currents may show wrong currents at the number 1, but it may be due to poor accurate altimetry data in the coastal waters (Gómez-Enri et al., 2008 ; Vignudelli et al., 2011). Cold waters at the number 2 may have less speed than the number 3 or may be, due to the opposite surface currents, were not able to continue their path. Contrary to these, water at the number 3 could penetrate into the middle of the sea, after these waters passed through the number 3, they are engaged and turned by two eddies and were not capable enough to continue their path into the middle of the sea.

These two eddies are shown by estimated geostrophic currents at numbers 4 and 5 (Figure 4b), in other words, torsion curved cold water indicates an eddy. Earlier, we said that warm waters of the southern Caspian Sea move toward the north in a straight line and enter the eastern coastal waters. Number 6 shows these warm waters that try to penetrate into cold waters of the eastern coasts and cold waters of upwelling procedure move toward the south and are shown in number 7 (Figure 4a). Eddies cause to turn the surface waters and this turn is identified in the SST image, for example, in Figure 5a there is an eddy near the coast (in

location A) that absorbed the waters and forced them to go into its inside. The waters which move to the south along the coasts are captured and turned by this eddy. The geostrophic currents show this eddy in location A (Figure 5a). The temperature difference between the inside and outside waters (the western waters) of eddy shows that adjacent waters cannot enter this eddy easily. Because the temperature of the eddy is close to the temperature of coastal waters, we can say just coastal waters enter the eddy.

Figure 5b shows another sample of an eddy that turns a narrow current of cold water around itself. Some selected vectors on a narrow path, which carries cold waters show abysmal and rotatory motion. According to what we have shown, warm waters of the southern Caspian Sea move toward the north and an example of it is shown on the eastern coasts in Figure 3. Another example is on the western coasts that a narrow flow of warm water is parallel and coincident with SLA contour lines (curve line of -0.45 meter in Figure 6b), and they moved in a curved path toward the north. Figure 6a shows the geostrophic currents and selected vectors show this curved path, and Figure 6b shows the SLA contour lines.

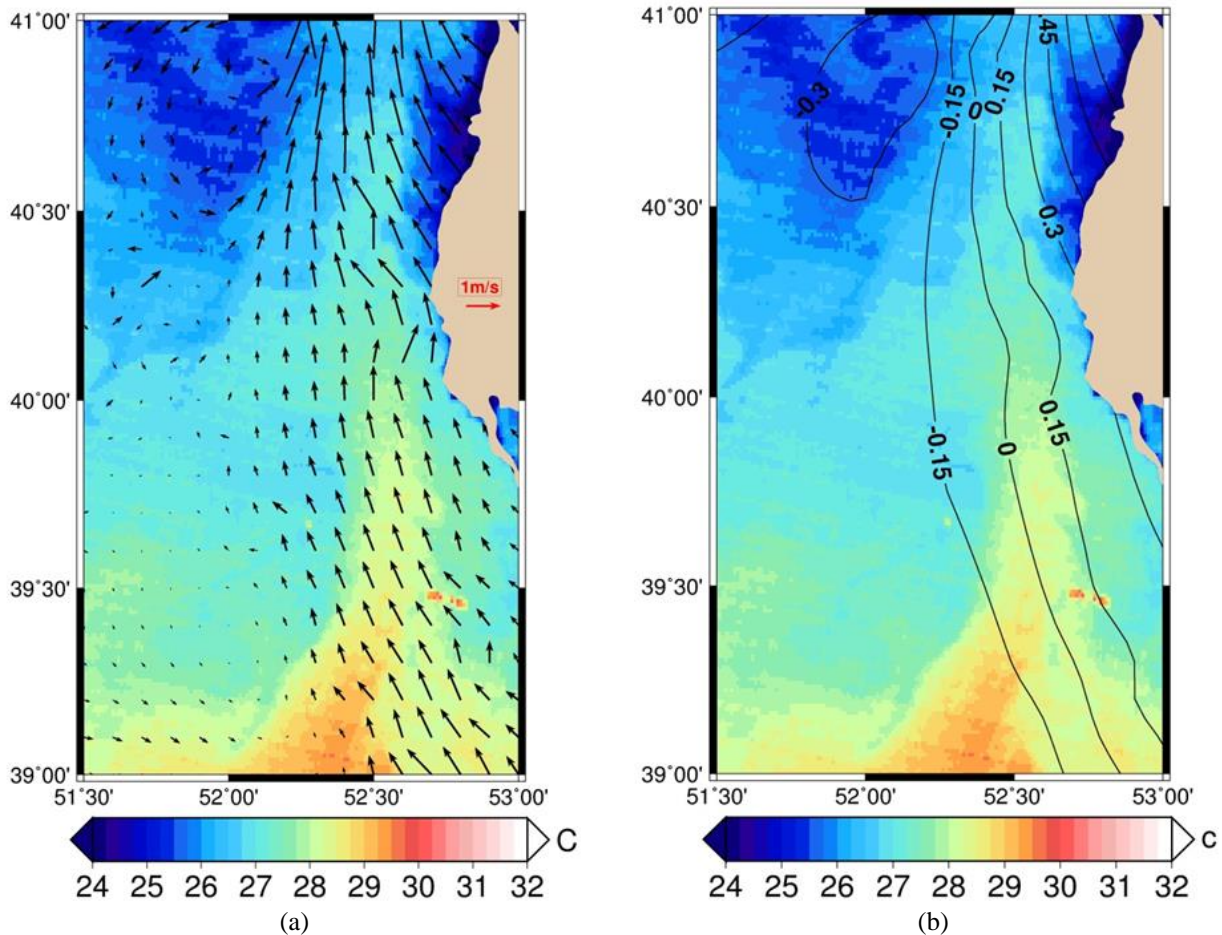


Figure 3. (a) Geostrophic currents and SST surface and (b) contour lines of SLA and SST surface

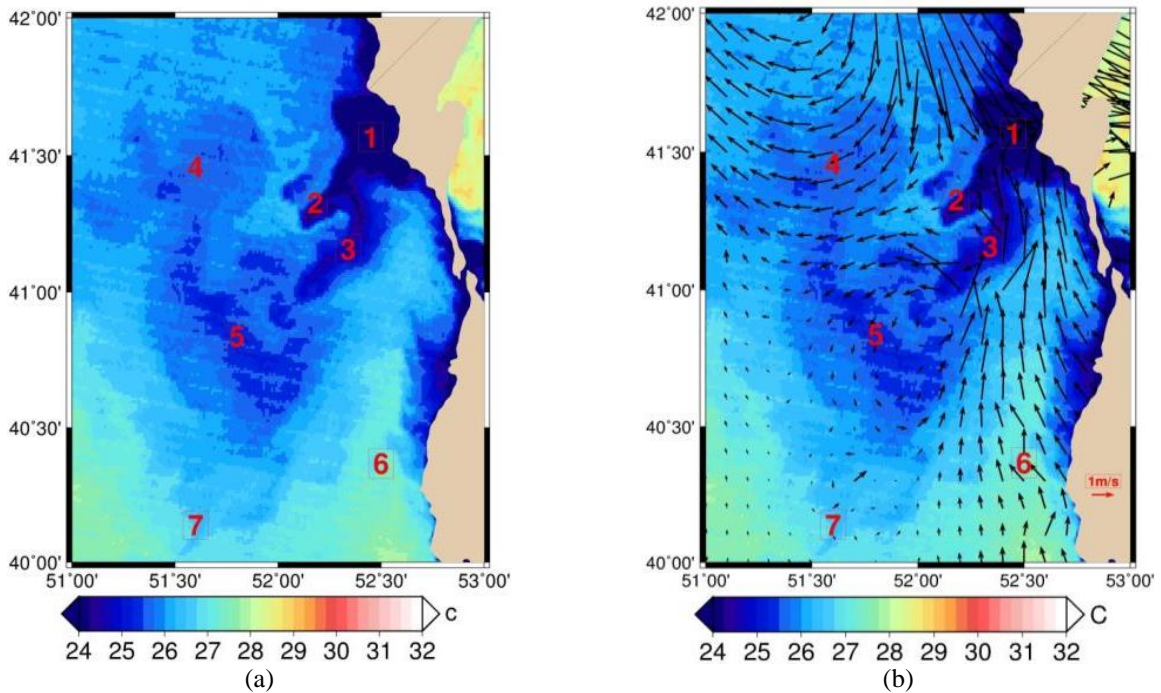


Figure 4. (a) SST image in the eastern coast of the Caspian Sea with seven specified areas and (b) Geostrophic currents and SST surface

4.2 Optical flow and SST

The results of this part include the optical flow calculated from two sequential SST images and the geostrophic currents estimated by altimetry along-track data from multi-missions in a period of five days (2010-07-31 to 2010-08-04) and mapped on the SST image (was taken on 2 August 2010 at 23:10). Two SST imageries in a day are selected and downloaded for optical flow process. The first image is on 2nd of August 2010 at 09:35 in the morning (Figure 7a), and the second image is on the same day at 23:10 (Figure 7b), and both were taken by Aqua satellite. These two SST images are as input for the optical flow (Horn & Schunck, 1981) algorithm and, calculate the displacement of SST or thermal patterns. According to previous studies, the along-

shore currents move toward the south along the eastern coasts (Vignudelli et al., 2011) and both optical flow (Figure 8a) and geostrophic currents (Figure 8b) show these currents, also another point is an eddy which is shown in both Figures (8a and 8b). In Figure 8a, there is a convergence of currents, which can be an eddy because it is likely that the eddy current absorbs the water into its center. Furthermore, there is an eddy that is shown in Figure 8b, but the eddy's location is slightly different from what is mentioned in the results of optical flow, and this may be due to lack of altimetry data. In Figure 9, the optical flow and the geostrophic currents are mapped on SST and SLA surface respectively, and they are a proof to show that optical flow results (Figure 9a) are the same as the direction of geostrophic currents (Figure 9b).

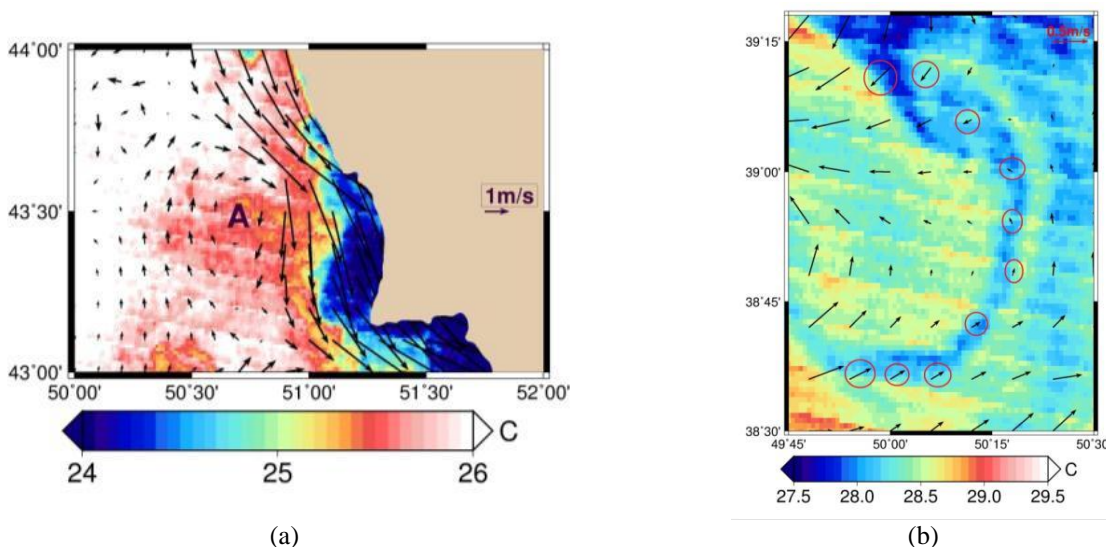


Figure 5. (a and b) The geostrophic currents, showing an eddy, mapped on SST image, respectively, in eastern and western coastal waters of the Caspian Sea

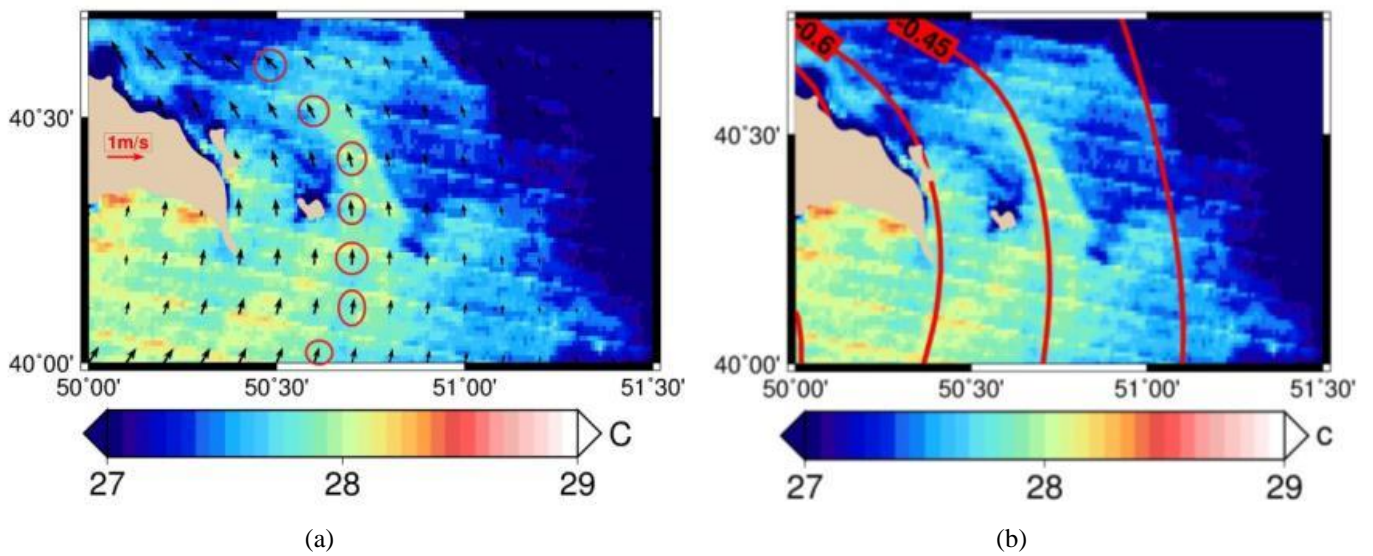


Figure 6. (a) Geostrophic currents and SST surface and (b) contour lines of SLA and SST surface

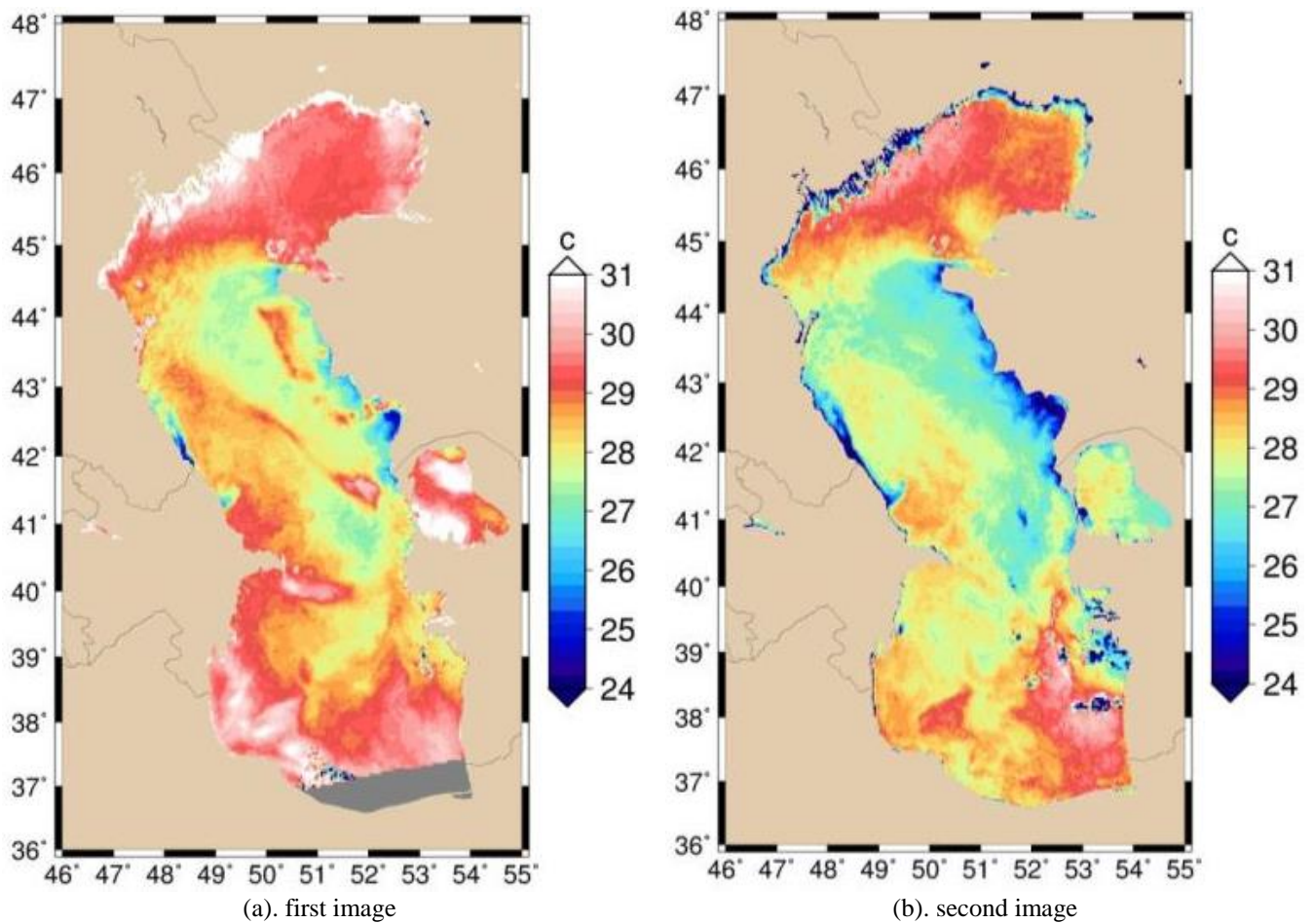


Figure 7. (a) SST image was taken by Aqua on 2 August 2010 at 09:35 (as the first image for optical flow process) and (b) SST image was taken by Aqua on 2 August 2010 at 23:10 (as the second image for optical flow process)

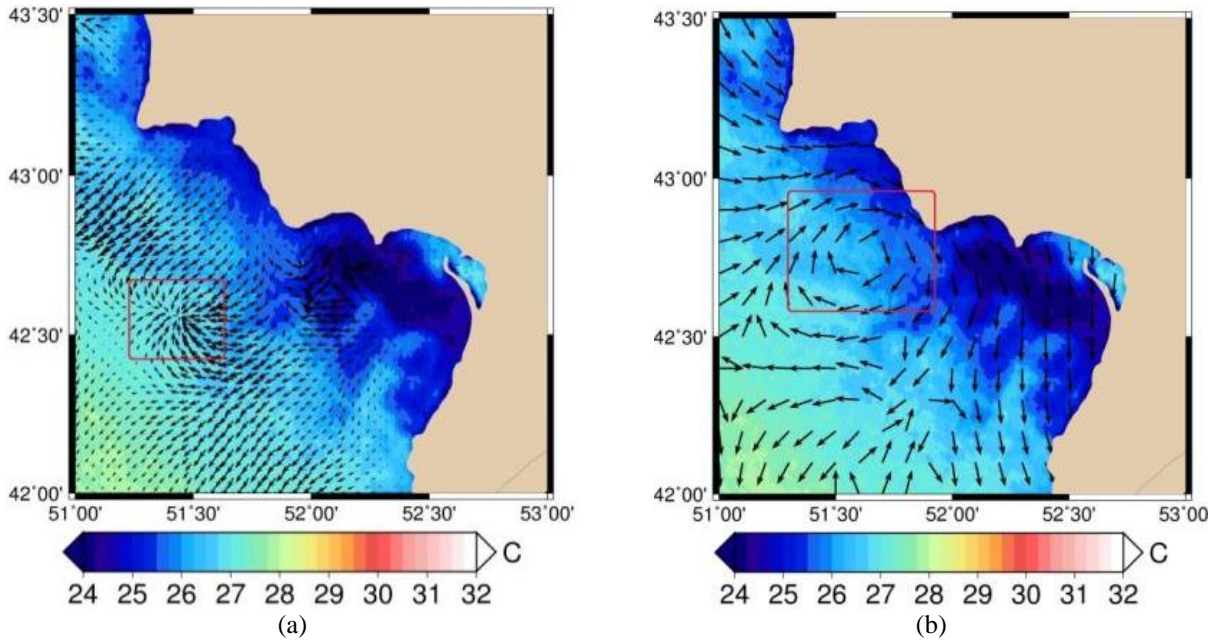


Figure 8. (a) Optical flow results and SST surface and (b) geostrophic currents and SST surface

In other words, Figures 9a and 9b show both flows move from the East to the West in a small area and then divide into two flows, one flow moves toward the north and the other moves toward the south, and this shape is clear in both optical flow and geostrophic currents. Optical flow in Figure 10a shows convergent flow and it can be an eddy, which geostrophic currents also show it (Figure 10b), but in fact, the reason that optical flow shows a convergent flow refers

to the structure of its equations. The optical flow algorithm intends to trace pixel values of first SST image (SST values) and find the corresponding of each pixel in the second SST image, and we know that in an eddy, image pixels move into the center of it, so clearly the optical flow vectors are directed toward the center of the eddy.

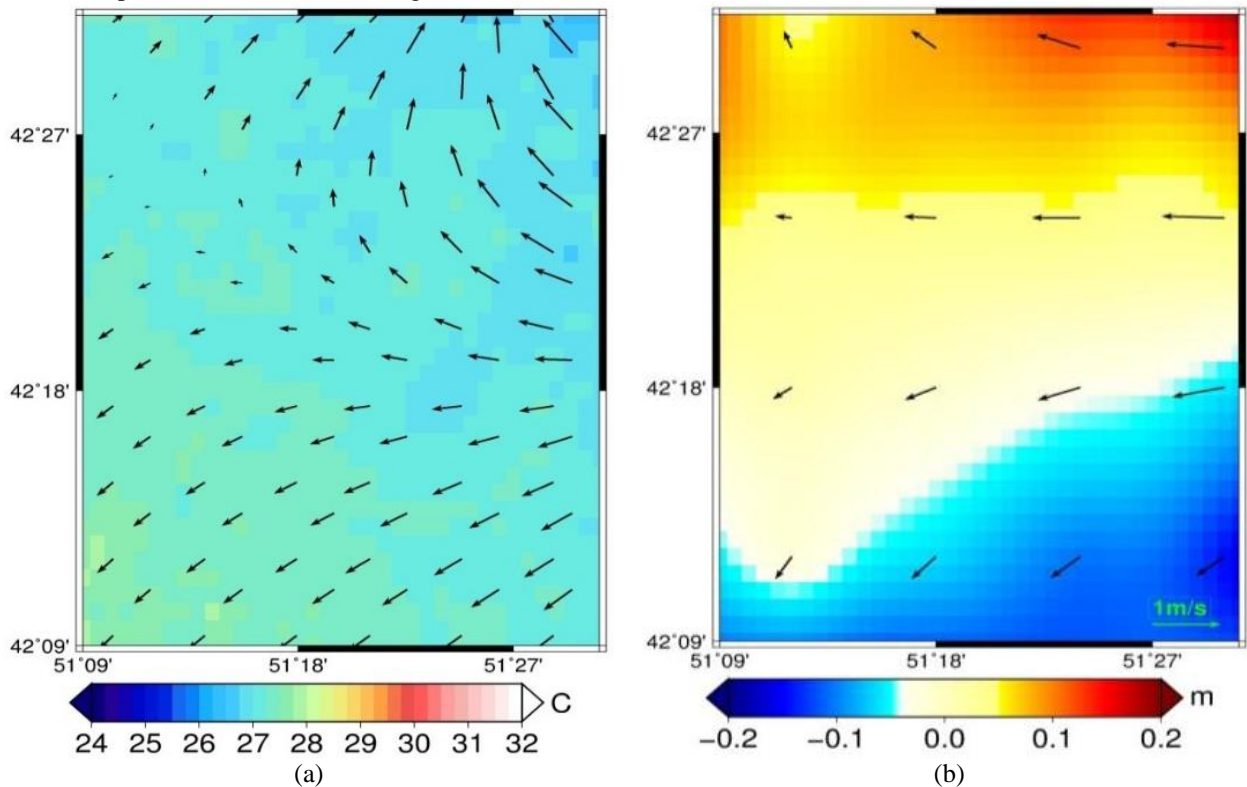


Figure 9. (a) Optical flow results mapped on SST surface and (b) Geostrophic currents mapped on SLA surface

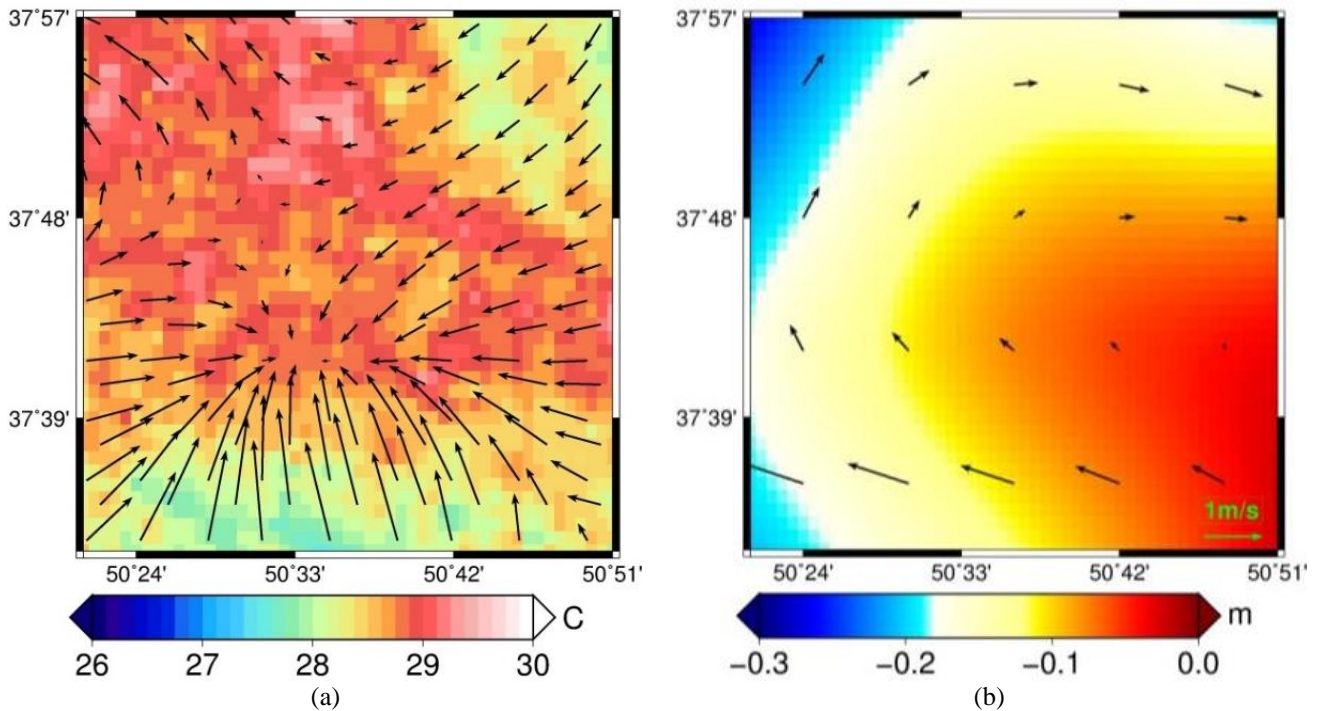


Figure 10. (a) Optical flow results mapped on SST surface and (b) Geostrophic currents mapped on SLA surface

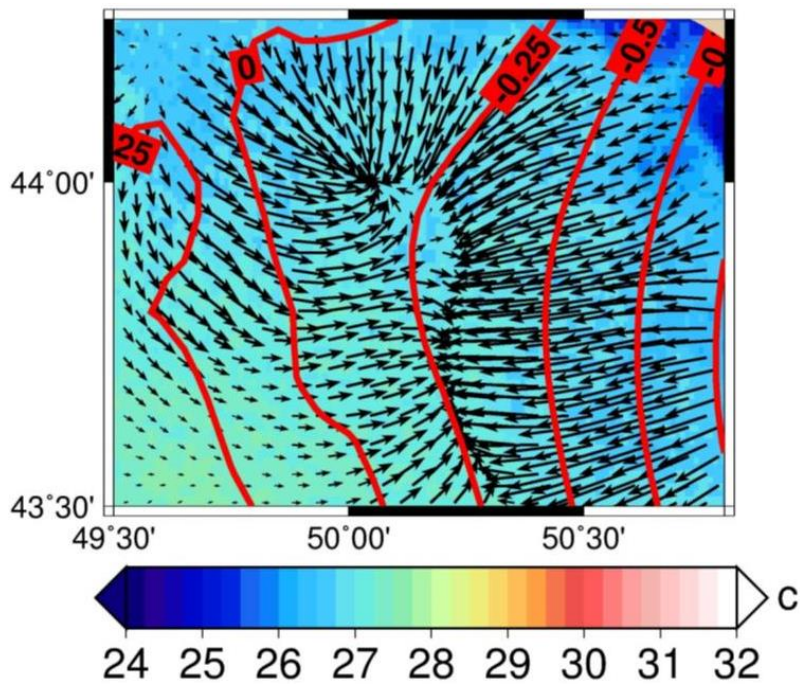


Figure 11. Optical flow results that are mapped on SST surface

Table 1. Angular differences between Optical flow and geostrophic currents (in deg.)

NW	N	NE
Avg: 1.05, std: 0.93	Avg: 1.17, std: 0.89	Avg: 1.06, std: 0.87
W	C	E
Avg: 1.86, std: 0.82	Avg: 1.21, std: 0.92	Avg: 1.25, std: 0.94
SW	S	SE
Avg: 1.27, std: 0.77	Avg: 1.33, std: 0.95	Avg: 1.01, std: 0.63

Due to Figure 11, it is clear that optical flow results (mapped on SST) converged on a line parallel to SLA contour lines. This line is very close to the level of zero at SLA contour lines. So, it might be concluded that sea surface currents are inclined to be balanced in SLA maps. To evaluate the result, we calculated angular differences between the optical flow and geostrophic currents in Figure 9. This calculation is processed by Arcos function as it can be calculated the angular differences between two vectors in range of 0 to 180 deg. The angular differences between each optical flow vector and the nearest geostrophic vector are calculated and shown in Table 1. The Figure 9 is divided into 9 small zones to estimate each difference in each zone and the average of the angular differences in each part is presented in Table 1.

5. Conclusion

The application of Horn-Schunck algorithm was investigated to estimate the SSCs and compare with geostrophic currents in various parts of the Caspian Sea. The main point in this article was observing an eddy in SST image that can be mapped on optical flow and geostrophic results to see their validation. Thin steams of SST patterns were observed, which were parallel to SLA contour lines and coincident with geostrophic currents direction (Figure 3). It is also shown that rotating geostrophic vectors were discovered at places with curved SST patterns (Figures 5 and 6). Due to the inconsistency between optical flow and geostrophic currents in some regions (Figure 8), lack of altimetry data was introduced as its probable reason. In addition, a comparison test was conducted between the optical flow and the geostrophic currents in Figure 9 and the results were so compatible (Table. 1). Clearly, to better understand some phenomena and mechanisms shown in this study, we need further study and other (in situ and satellite) data such as wind direction.

References

Aladin, N., & Plotnikov, I. (2004). The Caspian Sea. Lake Basin Management Initiative Thematic Paper.

Barannik, V., Borysova, O., & Stolberg, F. (2004). The Caspian Sea region: environmental change. *AMBIO: A Journal of the Human Environment*, 33(1), 45-51.

Barron, J. L., Fleet, D. J., & Beauchemin, S. S. (1994). Performance of optical flow techniques. *International journal of computer vision*, 12(1), 43-77.

Bowditch, N., 2012. The American Practical Navigator. CreateSpace Independent Publishing Platform.

Barnes, B. B., & Hu, C. (2013). A hybrid cloud detection algorithm to improve MODIS sea surface temperature data quality and coverage over the Eastern Gulf of Mexico. *IEEE Transactions on Geoscience and Remote Sensing*, 51(6), 3273-3285.

Cohen, I., & Herlin, I. (1999). Non uniform multiresolution method for optical flow and phase portrait models: Environmental applications. *International Journal of Computer Vision*, 33(1), 29-49.

Ghalenoei, E., Hasanlou, M., Sharifi, M. A., Vignudelli, S., & Foroughi, I. (2017). Spatiotemporal monitoring of upwelled water motions using optical flow method in the Eastern Coasts of Caspian Sea. *Journal of Applied Remote Sensing*, 11(3), 036016.

Ghalenoei, E., Sharifi, M. A., & Hasanlou, M. (2015). Estimating and Fusing Optical Flow, Geostrophic Currents and Sea Surface Wind in the Waters around Kish Island. *The International Archives of Photogrammetry, Remote Sensing and Spatial Information Sciences*, 40(1), 221.

Gómez-Enri, J., Cipollini, P., Gommenginger, C., Martin-Puig, C., Vignudelli, S., Woodworth, P., ... & Villares, P. (2008). COASTALT: improving radar altimetry products in the oceanic coastal area. *Proceedings of SPIE-Remote Sensing of the Ocean, Sea Ice, and Large Water Regions*, 15, 71050J.

Gunduz, M., & Özsoy, E. (2014). Modelling seasonal circulation and thermohaline structure of the Caspian Sea. *Ocean Science*, 10(3), 459-471.

Horn, B. K., & Schunck, B. G. (1993). "Determining optical flow": a retrospective. *Artificial Intelligence*, 59(1-2), 81-87.

Hosoda, K., Murakami, H., Sakaida, F., & Kawamura, H. (2007). Algorithm and validation of sea surface temperature observation using MODIS sensors aboard Terra and Aqua in the western North Pacific. *Journal of Oceanography*, 63(2), 267-280.

Jin, F., Khellah, F. M., Fieguth, P. W., & Winger, L. (2001). Motion estimation of sparse, remotely-sensed fields. In *Electrical and Computer Engineering, 2001. Canadian Conference on (Vol. 2, pp. 1135-1138)*. IEEE.

Kawai, Y., & Wada, A. (2007). Diurnal sea surface temperature variation and its impact on the atmosphere and ocean: A review. *Journal of oceanography*, 63(5), 721-744.

Hasanloua, M., & Saradjianb, M. R. (2006). Water motion analysis in SST images using least squares methods. *ISPRS parameters*, 3(2), 1.

Marcello, J., Eugenio, F., & Marqués, F. (2007, July). Methodology for the estimation of ocean surface currents using region matching and differential algorithms. In *Geoscience and Remote Sensing Symposium, 2007. IGARSS 2007. IEEE International (pp. 882-885)*. IEEE.

Gade, M., Seppke, B., & Dreschler-Fischer, L. (2012). Mesoscale surface current fields in the Baltic Sea derived from multi-sensor satellite data. *International journal of remote sensing*, 33(10), 3122-3146.

Minnett, P. J., Brown, O. B., Evans, R. H., Key, E. L., Kearns, E. J., Kilpatrick, K., & Szczodrak, G. (2004, September). Sea-surface temperature measurements from the Moderate-Resolution Imaging Spectroradiometer (MODIS) on Aqua and Terra. In *Geoscience and Remote Sensing Symposium, 2004. IGARSS'04. Proceedings. 2004 IEEE International (Vol. 7, pp. 4576-4579)*. IEEE.

MODIS Web [WWW Document], 2016 NASA Homepage. URL <http://modis.gsfc.nasa.gov/about/> (accessed 10.3.14).

Sandwell, D. T. (1987). Biharmonic spline interpolation of GEOS-3 and SEASAT altimeter data. *Geophysical research letters*, 14(2), 139-142.

Saraceno, M., Strub, P. T., & Kosro, P. M. (2008). Estimates of sea surface height and near-surface alongshore coastal

currents from combinations of altimeters and tide gauges.
Journal of Geophysical Research: Oceans, 113(C11).

- Seppke, B., Gade, M., Dreschler-Fischer, L., 2012. SEA SURFACE CURRENT FIELDS IN THE BALTIC SEA DERIVED FROM MULTI-SENSOR SATELLITE DATA. *Int. J. Remote Sens.* 33, 3122–3146. doi:10.1080/01431161.2011.628711
- Stammer, D., Wunsch, C., Giering, R., Eckert, C., Heimbach, P., Marotzke, J., & Marshall, J. (2003). Volume, heat, and freshwater transports of the global ocean circulation 1993–2000, estimated from a general circulation model constrained by World Ocean Circulation Experiment (WOCE) data. *Journal of Geophysical Research: Oceans*, 108(C1).
- Stewart, R. H. (2008). *Introduction to physical oceanography*. Robert H. Stewart. Chicago
- Vennell, R., & Beatson, R. (2009). A divergence-free spatial interpolator for large sparse velocity data sets. *Journal of Geophysical Research: Oceans*, 114(C10).
- Vignudelli, S., Kostianoy, A. G., Cipollini, P., & Benveniste, J. (Eds.). (2011). *Coastal altimetry*. Springer Science & Business Media.